The structure of electronic states in amorphous silicon

David A. Drabold,* Uwe Stephan,† Jianjun Dong,‡ and Serge M. Nakhmanson*

*Department of Physics and Astronomy, Ohio University, Athens, OH 45701-2979, USA
†Beckman Institute for Advanced Science and Technology, University of Illinois, Urbana, IL 61801, USA
‡Department of Physics and Astronomy, Arizona State University, Tempe, AZ 85287, USA

We illustrate the structure and dynamics of electron states in amorphous Si. The nature of the states near the gap at zero temperature is discussed and especially the way the structure of the states changes for energies ranging from midgap into either band tail (Anderson transition). We then study the effect of lattice vibrations on the eigenstates, and find that electronic states near the optical gap can be strongly influenced by thermal modulation of the atomic positions. Finally, we show the structure of generalized Wannier functions for amorphous Si, which are of particular interest for efficient ab initio *calculation of electronic properties and forces for first principles dynamic simulation. © 2000 by Elsevier Science Inc.*

INTRODUCTION

The electronic states of amorphous semiconductors are of both fundamental and applied interest. In this article we illustrate three aspects of the electronic states: We begin by discussing the zero temperature (equilibrium) electronic structure of a-Si. We do this for a very large (4 096-atom) model of a-Si in pleasing agreement with structural, vibrational, and electronic/optical properties at the same time. The nature of the electron states near the gap is elucidated by direct calculation, and we find that the states are very complex. These visualizations enable a qualitative understanding of the Anderson transition; in simple terms this amounts to understanding how the structure of the electron states evolves from localized (near the middle of the gap) to extended (well into either conduction or valence bands). Next, we put the electrons and classical lattice vibrations together; we show that the electronic band tail states experience a very large electron–phonon coupling that strongly affects the transport and optical properties of the material. Finally, we present detailed calculations for Wannier-like functions that are well localized in real space, and that span the occupied electronic subspace for the amorphous silicon models. These functions have special importance for current computational techniques (since they enable far more efficient calculations than are achieved by working directly with eigenstates, which are typically extended throughout the model).

BAND TAIL STATES AND THE ANDERSON TRANSITION AT ZERO TEMPERATURE

Since the seminal work of Anderson[1] it has been known that disorder induces localization of electron states. The detailed understanding of this has been a field of tremendous activity in condensed matter theory. In the parlance of amorphous semiconductors, the nature of the electron localization is determined by the microscopic structure of the band tail and midgap eigenstates and the dependence of this structure on the energy of the state. In this section, we report the explicit microscopic calculations of the band tail states using a very large and realistic 4 096-atom model of a-Si (a cube about 43 Å on a side), generated by Djordjevic et al.[2] A related calculation for amorphous diamond has been published.[3] This work goes well beyond related earlier work[4] on 216 or fewer atom cells, which accurately modeled deep gap states, but was limited in their ability to model *tail* states.

A localized-to-extended[1,5] transition occurs near both the valence and conduction band tails in a-Si, since midgap states are bound to be Anderson localized in a realistic model of a-Si and, likewise, states well into the valence or conduction bands (beyond the mobility edges) are extended. While this picture is certainly valid, it is also qualitative, and details, such as the

---

Corresponding Author: David A. Drabold.
E-mail address: drabold@ohiou.edu (D.A. Drabold)

exact nature of the mobility edge, are still controversial.[6] Within finite-size limitations of our model, we indicate qualitative features of the transition that are robust and salient to real a-Si, and that we suspect are relevant to any topologically disordered insulator.

The approximations of this section are as follows: (1) an orthogonal tight-binding Hamiltonian[7] with one s and three p basis functions per site and (2) the 4 096-atom supercell model of a-Si proposed in Ref. 2. The tight-binding model is an imperfect means of modeling electronic structure, but calculations[4] demonstrate that the qualitative features of the localization of electronic states due to disorder and their qualitative placement compare well with experiment, or with more sophisticated theory.[8]

The density of states for the Hamiltonian matrix is reproduced in the top panel of Figure 1 (Figure 1a): the global structure of the density of states is shown in the inset.[9] The valence edge shows more tailing than the conduction edge: This is consistent with experiments,[10] and theory,[11] which show that the valence tail is primarily due to structural disorder, while the conduction tail is much more sensitive to temperature, and originates in thermal disorder. Since this is a zero temperature calculation, the relatively greater width of the valence tailing is to be expected. The solid curve of Figure 1a is the maximum entropy fit to the density of states, and is quite exponential, similar to what we observed in amorphous diamond.[3] The decay parameter E_0 [such that density of states $\rho(E) \sim \exp(-E/E_0)$] is 190 meV. In earlier calculations on 216 or fewer atom cells, there are simply too few states to obtain a reasonable sampling of the band tail energy range.[4,12]

Next, we computed 500 midgap and band tail electronic eigenstates in the energy range between −0.5 and 1.5 eV, essentially exactly using the Lanczos[13] scheme. The position and localization of the individual states are reported in Figure 1b. Each spike indicates an energy eigenvalue, and the height of the spike is the localization from the inverse participation ratio (IPR): $I(\psi_n) = N\Sigma_{i=1}^{N} a_{ni}^4/(\Sigma_{i=1}^{N} a_{ni}^2)^2$, where $\psi_n = \Sigma_{i=1}^{N} a_{ni}\phi_i$ is the nth eigenvector and ϕ_i is one of the N orthogonal (tight-binding) basis orbitals. The IPR for ideally extended states is near 1.0 and an ideally localized state (on one basis orbital) would yield $I = N$. Figure 1b shows a smooth falloff in IPR as energy (doping) changes from midgap (say, near 0.5 eV) into the valence tail (near 0.0 eV). If the exact positions of the eigenvalues from Figure 1b are fit to an exponential form for the tail (dashed curve in Figure 1a), we get almost exactly the same tail as from maximum entropy. In Figure 1c, we estimate the DC conductivity using the Kubo formula,[14] where in this plot, the abscissa indicates the position of the Fermi level and the predicted conductivity from the states discussed in Figure 1b. We note that (1) the midgap states are incapable of carrying current since they are localized and sparse in the energy gap, (2) if the states become dense (and extended) enough, a nonzero conductivity is obtained when the model is doped to a Fermi level near $E = 0$, and (3) the conductivity rises *smoothly* with increasing p-doping.

To study the spatial structure of electron states and the qualitative nature of the local-to-extended transition, we "visualize" states by assigning different colors to every atom according to the "charge" associated with the atom site for a given eigenstate. In Color Plate 1, we choose six typical valence states. The positions of these states are also cross-labeled as (a)–(f) in Figure 1b. For the effect of visualization, only 75%
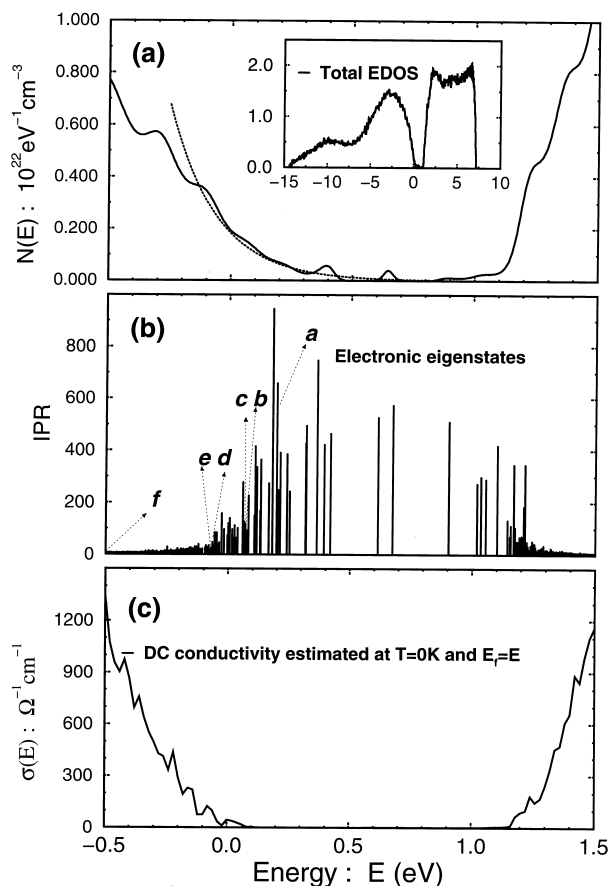

Figure 1. Electronic states in the band-gap region: (a) Electronic density of states (DOS) computed by maximum entropy technique. The total DOS is condensed in the encapsulated graph. Four hundred moments and 50 random vectors were used (Ref. 9). The valence band tail is approximately exponential with width of 190 meV as estimated with a fitting function (dashed line). (b) Energies and localization (from inverse participation ratio [IPR]; see text) of gap states from Lanczos calculation. Large IPR implies more spatial localization. The letters illustrate the location in energy of the eigenstates depicted in Color Plate 1. (c) The estimated DC conductivity as a function of doping (location of the Fermi level) computed with the Kubo formula.

charge in each state is shown (those atom sites contributing less charge density are omitted). Changes in color thresholds modify the detailed appearance, but the features we discuss are robust to sensible changes in the visualization. Color Plate 1a is a typical exponentially localized state in which the "charge" is confined to a small cluster of atoms near a major structural distortion (bond angles severely deviating from tetrahedral bonding). The size of the cluster increases as the energy is tuned from midgap toward valence band (it is not perfectly monotonic). For energies deeper into the valence band ($E < 0.1$ eV), the eigenstate "proliferates" into a form consisting of several small clusters. At the beginning of this phase, an energy eigenstate is composed of two clusters weakly overlapping each other in real space. This is seen in Color Plate 1b and c.

This could be understood with perturbation theory: two nearly energy-degenerate localized clusters weakly overlapping each other will admix to form two new states. Deeper into the tails there are many overlapping clusters (see e.g., Color Plate 1d and e). Our qualitative picture of the local-to-extended transition in a-Si, based on our detailed calculations, is the following: As severe distortions are rare, clusters stemming from such distortions are probably isolated from each other and, if isolated, are localized energy eigenstates. For less severe distortion, the probability of occurrence increases, and the size of associated clusters is also larger. Then the chance of finding another cluster of similar energy in the neighborhood increases. As the distortion becomes less severe, two, three, or more clusters could mix together. At some point, clusters can always find "overlapping energy partners" and they mix together to enable electronic connectivity. This state of affairs can be identified with the "mobility edge." In some ways, our model resembles results from classic percolation theory for conductivity.[15] We discuss this model fully elsewhere.[16]

THERMAL EFFECTS ON THE ELECTRONIC STATES

In this section we add thermal disorder to the structural disorder and investigate the resulting fluctuations in the electron states, the structure of which is modulated by the lattice vibrations.[17] These fluctuations in structure of the eigenstates occur *only* if there are localized energy states adjacent both within energy (meaning within a few tenths of an electron volt), and real space, and such that the thermal disorder at a given temperature is sufficient to occasionally bring the energy eigenvalues of the adjacent states very close together. These conditions are often met in realistic models of a-Si for states near the Fermi level at room temperature. Thus, the picture that emerges is one in which the energy eigenvalues and sites where those eigenstates are localized change rapidly and drastically in a quasioscillatory (but not periodic) manner. Further, the sites where a state is most localized may form wandering stringlike structures or columns where no two favored sites are nearest neighbors. However, in a variety of physically relevant temperature and energy ranges states never form a static structure, and often a spherical approximation for their geometry would be inappropriate. This is very different from the prevailing view. While we have limited the current study to a-Si, there is every reason to believe that the qualitative picture we present here is suited to any disordered insulator, such as glasses.[18] Unfortunately it is very difficult to directly connect these results to experiments because the time scales are very short; yet the ideas contained here are important to constructing proper theories of transport and optical effects.

This work complements an important body of existing theory work. Phenomenological theories of defect dynamics and kinetics (the defect pool model[19]) and transport[6] have solved outstanding problems in their respective areas in a-Si and glasses. A value of the present work is to elucidate the foundations of these approaches by describing *explicitly* the nature of the electron states and their short-time dynamics. It is hoped that this will enhance and extend the value of these theories, and perhaps enable "*ab initio*" input to the phenomenological models.

In this section we employ the approximate local basis *ab initio* molecular dynamics scheme of Sankey and Niklewski.[8] The method is tested for Si in many forms and is quite reliable. As in previous sections, we start with relaxed versions of the supercell structural models of Djordjevic et al.,[2] which are currently the most realistic models of a-Si extant since they are the only ones to our knowledge that simultaneously reproduce structural, electronic/optical,[20] and vibrational properties of a-Si. In this section we limit ourselves to 216- and 512-atom models.

In Figure 2 we indicate the time dependence of the LDA eigenvalues in the vicinity of the optical gap. The Fermi level is near the middle of the gap and several states near the Fermi level are appropriately described as band tail states. These are much like the states that would be responsible for conduction in doped a-Si:H. Figure 2a and b illustrates the effect for a simulation at 300 and 150 K, respectively. As in earlier work[21,22] there is a roughly linear relation between RMS temporal fluctuation and temperature. As expected, the higher
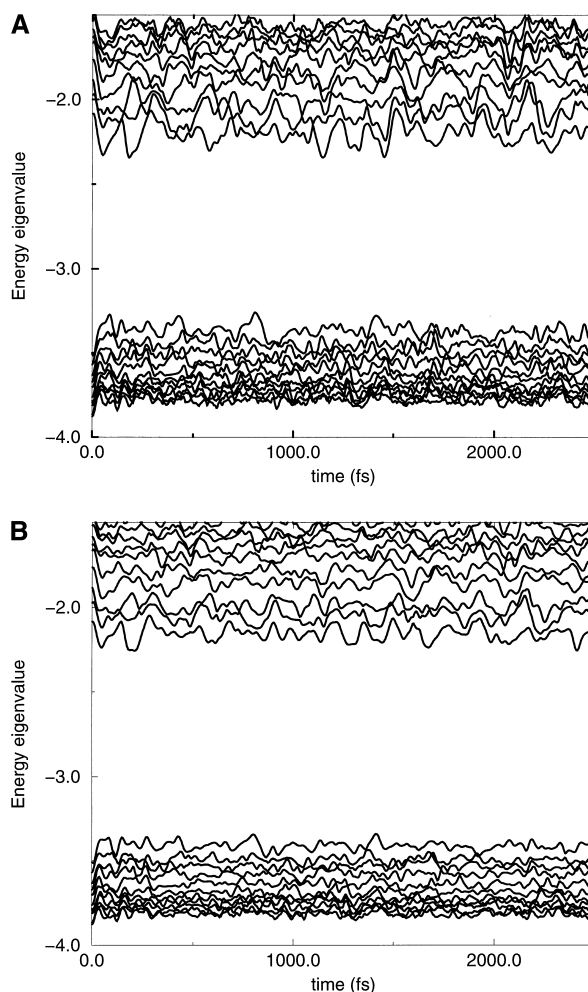

Figure 2. Approximate LDA energy eigenvalues plotted against time (in femtoseconds) for 216-atom model[2] 300 K thermal simulation. The Fermi level is in the middle of the optical gap (near −2.7 eV). Note the large thermal fluctuations in the eigenvalues near the gap, and the occasional close approach of neighboring energy eigenvalues. (a) Simulation at 300 K; (b) 150 K (see text).

temperature simulation leads to larger excursions in the positions of the energy eigenvalues. Note for Figure 2a (300 K) that the lowest unoccupied molecular orbital (LUMO) fluctuates in time by about ~0.3 eV, much larger than thermal energies (~10 meV). States deeper into either the valence or conduction bands show progressively less thermal modulation because they are less localized (we have noted[18] a very strong correlation between the rms fluctuation in the energy eigenvalues due to thermal disorder and the inverse participation ratio, a simple measure of localization in the $T = 0$ model). The localization "amplifies" the electron–phonon coupling. Also, the conduction states fluctuate more than the valence states (suggesting that the conduction tails are more sensitive to thermal disorder than the valence tails, which originate primarily from structural disorder), in pleasing agreement with total yield photoemission experiments[10] and earlier theory work.[11,22]

The key conclusions of this article can be inferred from Color Plate 2, in which we illustrate "snapshots" of a particular electronic eigenvector (the LUMO state) extracted from a 300 K simulation of a-Si.[21] In Color Plate 2, different colors indicate different levels of charge on a given atom (the ordering is red, green, blue, gray, white; see the caption to Color Plate 2 for detail). There is a clear tendency for the LUMO state to alternately "accumulate" on a strained part of the network, sometimes becoming strongly localized (Color Plate 2a), but also occasionally developing a substantially more extended "stringlike" character (Color Plate 2b). These are not the only two recognizable structures, but recur most frequently. The time between "characters" is not predictable, although it is on the order of tens of hundreds of femtoseconds.

In Figure 3, we reproduce the 300 K temporal fluctuations of the LDA eigenvalues near the gap for a larger (512-atom) model of a-Si also made by Djordjevic et al.,[2] and also in excellent uniform agreement with experiments. This larger model illustrates some additional points. Although the LUMO energy level fluctuates considerably, the structure of its conjugate eigenvector is much more "static" than the LUMO state of Color Plate 2. Even though there is obviously a large electron–
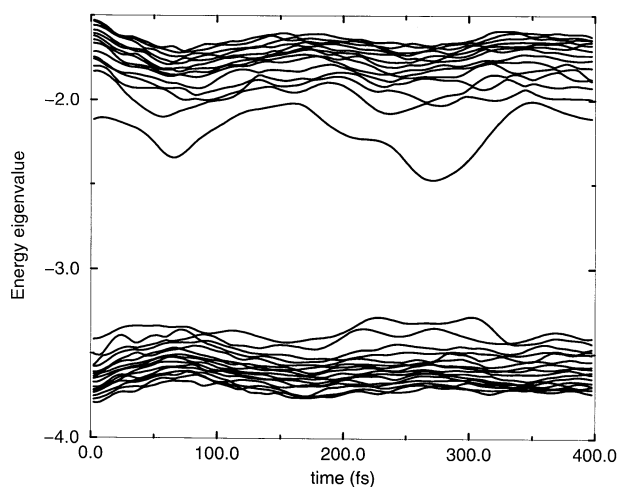
phonon coupling (because of the large fluctuations in energy), the state does not approach closely enough to the next conduction state in energy to exhibit strong mixing and therefore markedly change its structure. This emphasizes the point that a large electron–phonon coupling by itself is not sufficient to cause major changes in the structure of the relevant eigenvector. In Color Plate 3, we illustrate the highest occupied molecular orbital "HOMO" state and snapshots in analogy with Color Plate 2. By inspection of the time development of this state from Figure 3, there are two "close approaches" of this state to the next valence tail state. Indeed, we find that the qualitative behavior of this state is similar to that from Color Plate 2, "snapshots" with color coding identical to Color Plate 2 are presented as Color Plate 3a and b, illustrating compact cluster and chainlike character, respectively. In the short simulation for the 512-atom model (400 fs), we also saw a distinctive structure involving three rather separated clusters. We conclude that the phenomenon is qualitatively similar for occupied levels such as this or for unoccupied states (the LUMO of Color Plate 2).

We have argued earlier[16] that structural disorder in a-Si gives rise to localized states with energies in the band tails. This work[16] showed that it is useful to view localized energy eigenstates in a-Si as either pure or mixed "cluster states." Cluster states are localized eigenstates of an idealized system that stem from some structural irregularity such that there is no overlap with energetically degenerate clusters. Such cluster states can be difficult to realize in isolation in real a-Si, since structural defects can occur with similar local electron energies, which would cause the system energy eigenvectors to consist of mixtures of the resonant defect clusters if the defects are in adequate spatial proximity to allow overlap between cluster states. We have explained this in Ref. 16. The "simple physics" of this article is that the strong electron–phonon coupling for localized band tail states is sufficient to cause strongly time/temperature-dependent quantum mechanical mixing of cluster states when the thermal disorder is "just right" to make their energies nearly degenerate provided that they have some overlap in real space. Strong mixing of course implies less localization and thus better prospects, at least while the more extended state survives, for conductivity and optical transitions. This work shows that transport and optical calculations based only on $T = 0$ results can be quite misleading.

The consequences of this work can be stated another way. If $|i\rangle$ ($|f\rangle$) are initial (final) electronic states with energy E_i (E_f), then for an electronic transition in a-Si, a Fermi golden rule argument leads quickly to the conclusion[5] that the transition rate is proportional to $|\langle i|\hat{T}|f\rangle|^2 \delta(E_f - E_i - \hbar\omega)$, where $\hat{T}$ is a perturbation inducing the transition (to first approximation a momentum operator) and ω is the frequency of an external probe. Both the energies in the δ function and the transition matrix elements are sensitive to the instantaneous details of the structural disorder, and as such transition probabilities are also strongly dependent on the time and temperature. The consequences of this to transport are under investigation; the discussion here is based on first-order time-dependent perturbation theory, which for the very strong electron–phonon coupling we discuss, could be inadequate.

Figure 3. Approximate LDA energy eigenvalues plotted against time (in femtoseconds) for 512-atom model[2] for 300 K thermal simulation. The Fermi level is contained in the gap (near −3.0 eV).

REAL-SPACE LOCALIZED REPRESENTATION FOR ELECTRONS: GENERALIZED WANNIER FUNCTIONS FOR AMORPHOUS SILICON

In this section, we discuss a different approach for electronic structure computations. This is the concept of using Wannier-like states, which are unitary transformations of the eigenstates of a given one-particle Hamiltonian. Although these states are not eigenstates by themselves, they can be used equally well to construct wave functions and therefore contain the same physics as the eigenstates. The freedom in the choice of the unitary transformations, however, allows one to select Wannier-like functions with special properties, e.g., functions that are to a maximum extent localized.[23] Of particular interest for electronic structure investigations are those localized Wannier-like functions that are created from all occupied eigenstates. These functions reflect the bonding properties of a given system and therefore can be used to describe and understand local physical and chemical properties of this system. In fact, the interest in such Wannier states has enormously increased during the last years as they form the basis for the so-called modern theory of polarization.[24]

From a computational perspective, the most natural approach to an *ab initio* (density functional) total energy or force calculation is to solve the time-independent Schrodinger equation for the eigenvalues and eigenstates. Then, for a given conformation, the challenging part of the total energy is given by the sum of the occupied energy eigenvalues. The difficulty with this approach emerges when one considers very large systems, such as the 4 096-atom model.[2] In particular, it is intuitively clear, for example, that the force on a particular site depends on the local environment of that site, not on an atom 1 μm away! The tool needed to reformulate the energy and force calculations locally is the real-space localized Wannier representation.

The explicit computation of Wannier-like states from eigenstates is feasible, however, only for systems that are not too large because the computation of a complete band of eigenstates scales with the third power of the system size. The locality of these functions, however, opens up a completely new and different way of extracting electronic properties from a one-particle Hamiltonian without computing eigenstates. These are methods that scale only linearly with the system size [so-called $O(N)$ methods]. In these methods, the locality of the Wannier states or the related density matrix is exploited to compute electronic quantities as traces, where the single terms in these traces are local and can be computed to a good approximation within confined regions of the whole system (so-called localization regions). Several such schemes have been proposed, including the Fermi operator expansion (or projection), method[25,26] the variational minimization of $O(N)$ energy functionals based on linearly independent or dependent Wannier-like states,[27] and the minimization of functionals that directly employ a density-matrix description.[28] Of all these methods, the projection method has the advantage of exhibiting a linear scaling also with respect to the size of the localization regions. This is important if large regions are required to achieve a high accuracy in the computations.

In this projection method, the density operator in the given system is represented as a polynomial (Chebyshev) approximation of the Fermi distribution function applied to the given Hamiltonian operator. This polynomial expansion can be recast in matrix form by using the so-called contracovariant or upper–lower indexed Hamiltonian matrix[26] H, which is the product of the inverse overlap matrix of the basis states used and the ordinary (lower indexed) Hamiltonian matrix: $\mathbf{D} = (\mathbf{S}^{-1})\mathbf{H}$.

At zero temperature, the resulting density operator can be used to project out Wannier-like functions from a given set of initial functions. In this case, however, the Chebyshev expansion will only approximately describe the step distribution function. The accuracy of this approximation depends on the size of the band gap—the smaller the gap, the more polynomial terms must be taken into account.

If one starts from as many (appropriately chosen) initial states as there are electron pairs in the system, the resulting projected functions are linearly independent and can be orthonormalized. These orthonormalized projected functions then have all the properties of Wannier-like states. To maintain the linear scaling of the method, we perform the orthonormalization also within localization regions that are, however, dynamically defined to maximally reduce the remaining overlap terms.[29]

Color Plate 4 shows one such orthonormalized projected Wannier-like function in the tetrahedrally coordinated amorphous Si model containing 4 096 atoms. For these computations, we used the local-orbital LDA Hamiltonian of Sankey and Niklewski.[8] The atomic orbitals in this Hamiltonian are strictly set to zero outside a certain cutoff range (5.0 bohr radii for Si). Because of the complete fourfold coordination of the system, we could start with bonding orbitals as initial functions, which are bonding combinations of hybrid orbitals pointing in bond directions. Furthermore, we used fixed localization regions during the projection that contained all atoms within seven bond steps from the originating bond. These regions were then dynamically adjusted during the orthonormalization. (For the particular Wannier function shown, the final localization region contained 476 atoms.)

Color Plate 4 depicts the charge density of the resulting Wannier state within a plane defined by the two atoms that form the initial bond, and a third neighboring atom. The three atoms are indicated by small white crosses. The colors describe a logarithmic charge density plot with densities reaching from its maximum value as shown in red through green and blue (blue for zero density outside the local regions). In addition, Color Plate 4 contains contour lines of equal charge density where the density logarithm crosses an integer value. The thick black lines, which are composed of many contour lines, represent node lines at which the Wannier function changes sign.

We selected the Wannier state at a bond at atom 32 of the Djordjevic et al. cell,[2] which was described earlier in this article. This atom has an extremely distorted environment as can be seen in Color Plate 4 from the position of the third atoms, which form a very small and a very large angle with the originating bond. These local distortions result in a sizable asymmetry of the Wannier state already in the immediate vicinity of the central bond. Nevertheless, the function is clearly localized and bonding at the originating bond, and is antibonding to the neighboring atom to fulfill the orthonormality constraint. When going out further in space, the function becomes highly irregular because of the disordered nature of the system. It oscillates several times until it reaches the boundary of the localization region. These boundaries are sharp
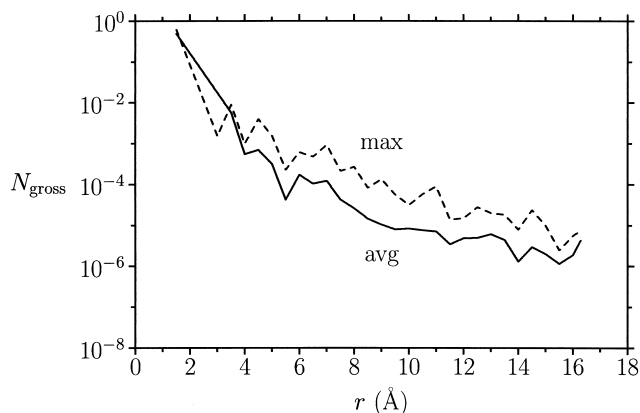
Figure 4. Decay of the Wannier function of Color Plate 4 as measured by the gross Mulliken populations as a function of radial distance from the bond center. The decay is approximately exponential up to large distances. "avg" means average over all populations at a given radial bin.

in the logarithmic plot because of the cutoff in the atomic orbitals. However, a very interesting feature visible in Color Plate 4 is that the resulting Wannier functions are far from being spherical. This is a result we had already found earlier using a simpler Hamiltonian.[26] The functions prefer to spread out in certain bond directions while they more quickly decay in other parts of their environment. The spatial decay of the state in Color Plate 4 is indicated in Figure 4.

An exponential decay is expected whenever the eigenstates that create the Wannier states (the occupied eigenstates in our case) are separated from the remaining (unoccupied) states by a gap. However, there is not yet a completely general proof for this statement. Therefore, explicit computations of Wannier functions together with their tails also open a way to a better understanding of the fundamental properties of these functions.

CONCLUSION

In this article we have shown the structure of typical current electronic structure calculations for a-Si. We have illustrated the character of the electron states at zero temperature near the Fermi level. The idea here is similar to the celebrated Anderson problem,[1] but with more "realistic" off-diagonal disorder originating from the topological disorder of a realistic and large model of a-Si. Then, we showed that the band tail states are very sensitive to additional disorder from lattice vibrations. This is very important for optical and transport calculations, and the defect pool model. On an important theoretical and computational note, we computed generalized Wannier functions for a-Si. Their existence is essential to enable really large-scale (several thousand atom) calculations by electronic structure methods.
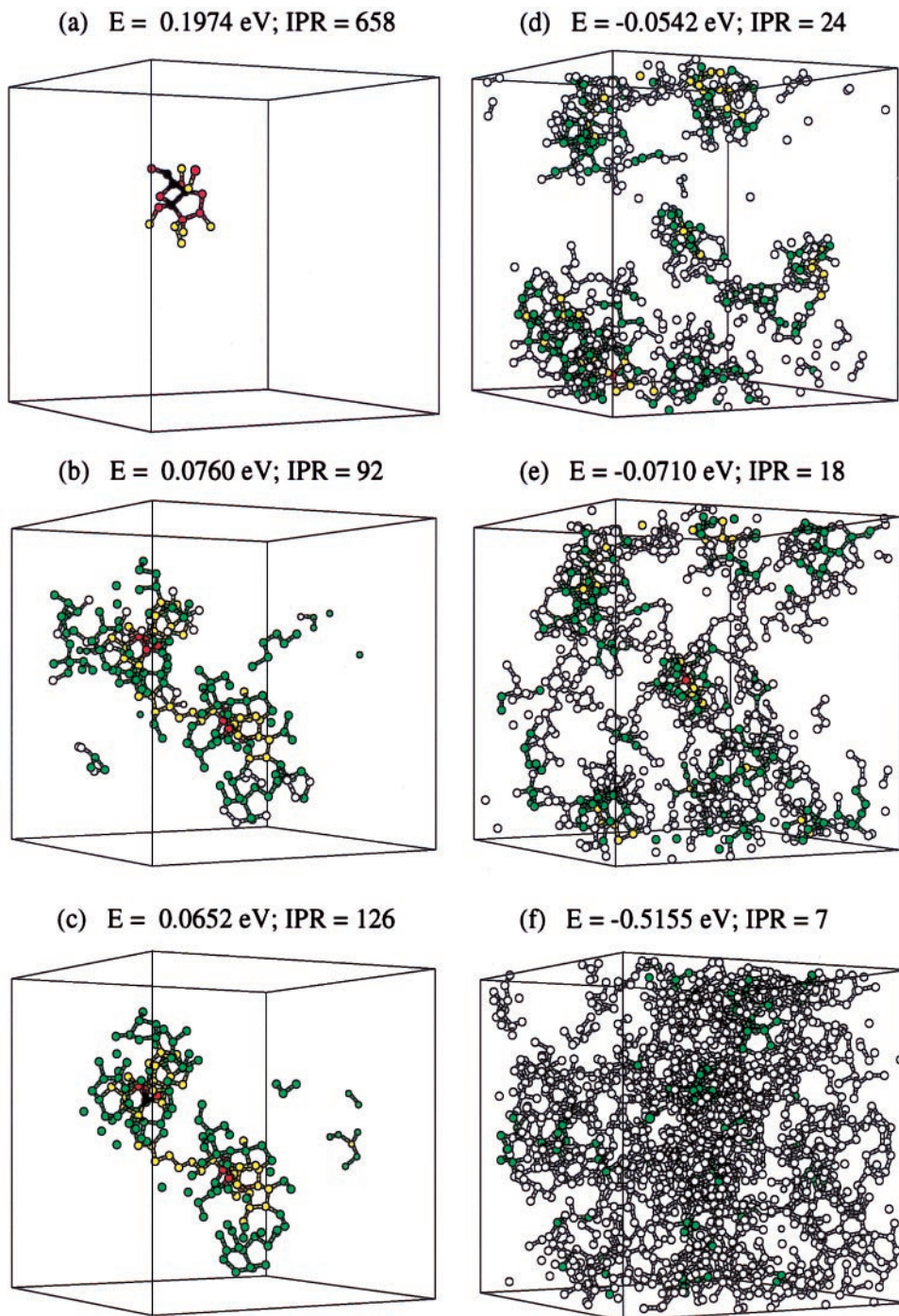
ACKNOWLEDGMENTS

REFERENCES

1. Anderson, P.W. Absence of diffusion in certain random lattices. *Phys. Rev.* 1958, **109,** 1492–1497
2. Djordjevic, B.R., Thorpe, M.F., and Wooten, F. Computer model of tetrahedral amorphous diamond. *Phys. Rev. B* 1995, **52,** 5685–5689
3. Dong, J., and Drabold, D.A. Band-tail states and the localized-to-extended transition in amorphous diamond. *Phys. Rev. B* 1996, **54,** 10284–10287
4. Mercer, J.L., and Chou, M.Y. Tight-binding study of the electronic structure of amorphous silicon. *Phys. Rev. B* 1991, **43,** 6768–6771; Nichols, C.S., and Winer, K. Localization of band-edge states in periodic models of a-Si. *Phys. Rev. B* 1988, **38,** 9850–9856; for a related Bethe lattice calculation, Fedders, P.A., and Carlsson, A.E. Energy levels and charge distributions of nonideal dangling and floating bonds in amorphous Si. *Phys. Rev. B* 1989, **39,** 1134–1139; Joannopoulos, J.D. Theory of fluctuations and localized states in amorphous tetrahedrally bonded solids. *Phys. Rev. B* 1977, **16,** 2764–2774
5. Mott, N.F., and Davis, E.A. *Electronic Processes in Non-Crystalline Materials.* Clarendon, Oxford, 1979
6. See, for example, Adriaenssens, G.J. Amorphous silicon: defects and disorder. In: *Amorphous Insulators and Semiconductors* (Thorpe, M.F., and Mitkova, M.I., eds.), NATO ASI Series. Kluwer, Dordrecht, 1997, pp. 437–468
7. Kwon, I., Biswas, R., Wang, C.Z., Ho, K.M., and Soukoulis, C.M. Transferable tight-binding models for silicon. *Phys. Rev. B* 1994, **49,** 7242–7250
8. Sankey, O.F., and Niklewski, D.J. Ab initio multicenter tight-binding model for molecular-dynamics simulations and other applications in covalent solids. *Phys. Rev. B* 1989, **40,** 3979–3995
9. Drabold, D.A., and Sankey, O.F. Maximum entropy approach for linear scaling in the electronic structure problem. *Phys. Rev. Lett.* 1993, **70,** 3631–3634
10. Aljishi, S., Cohen, J.D., Jin, S., and Ley, L. Band tails in hydrogenated amorphous silicon and silicon-germanium alloys. *Phys. Rev. Lett.* 1990, **64,** 2811–2814
11. Drabold, D.A., Fedders, P.A., Klemm, S., and Sankey, O.F. Finite-temperature properties of amorphous silicon. *Phys. Rev. Lett.* 1991, **67,** 2179–2182
12. Dong, J., and Drabold, D.A. Unpublished.
13. Golub, G.H., and Van Loan, C.F. *Matrix Computations.* Johns Hopkins University Press, Baltimore, 1983. A sophisticated and convenient implementation of the Lanczos method is due to M.T. Jones and M.L. Patrick, 1989; available from netlib as "lanz"
14. Thouless, D.J. Electrons in disordered systems and the theory of localization. *Phys. Rep.* 1974, **13,** 93–142
15. Zallen, R. *The Physics of Amorphous Solids.* John Wiley & Sons, New York, 1983
16. Dong, J., and Drabold, D.A. Atomistic structure of band-tail states in amorphous silicon. *Phys. Rev. Lett.* 1998, **80,** 1928–1931; for a clearer rendition of the states, see http://www.phy.ohiou.edu/~drabold/prl/prl.html
17. Drabold, D.A., and Fedders, P.A. Electronic consequences of the mutual presence of thermal and structural disorder. *Phys. Rev. B* 1999, **60,** R721–R725
18. Cobb, M., and Drabold, D.A. Ab initio molecular-dynamics study of liquid GeSe$_2$. *Phys. Rev. B* 1997, **56,** 3054–3065; and references therein

19. See, for example, Street, R.A. *Hydrogenated Amorphous Silicon*. Cambridge University Press, Cambridge, England, 1991

20. See Allan, G., Delerue, C., and Lannoo, M. Electronic structure of amorphous silicon nanoclusters. *Phys. Rev. Lett.* 1997, **78**, 3161–3164

21. For an mpeg format animation, see http://www.phy.ohiou.edu/~drabold/fluctuate.html

22. Drabold, D.A. Molecular-dynamics simulations of network glasses. In: *Insulating and Semiconducting Glasses* (Boolchand, P., ed.). World Scientific, Singapore, 1999 (in press)

23. Marzari, N., and Vanderbilt, D.H. Maximally localized generalized Wannier functions for composite energy bands. *Phys. Rev. B* 1997, **56**, 12847–12865

24. See, for example, Nunes, R.W., and Vanderbilt, D.H. Real-space approach to calculation of electric polarization and dielectric constants. *Phys. Rev. Lett.* 1994, **73,** 712–715

25. Goedecker, S., and Colombo, L. Efficient linear scaling algorithm for tight-binding molecular dynamics. *Phys. Rev. Lett.* 1994, **73,** 122–125; Sankey, O.F., Drabold, D.A., and Gibson, A. Projected random vectors and the recursion method in the electronic-structure problem. *Phys. Rev. B* 1994, **50**, 1376–1381

26. Stephan, U., and Drabold, D.A. Order-N projection method for first-principles computations of electronic quantities and Wannier functions. *Phys. Rev. B* 1998, **57,** 6391–6407

27. Ordejón, P., Drabold, D.A., Grumbach, M.P., and Martin, R.M. Unconstrained minimization approach for electronic computations that scale linearly with system size. *Phys. Rev. B* 1993, **48,** 14646–14649; Ordejón, P., Drabold, D.A., Martin, R.M., and Grumbach, M.P. Linear system-size scaling methods for electronic-structure calculations. *Phys. Rev. B* 1995, **51,** 1456–1476; Mauri, F., Galli, G., and Car, R. Orbital formulation for electronic-structure calculations with linear system-size scaling. *Phys. Rev. B* 1993, **47,** 9973–9976

28. Li, X.-P., Nunes, R.W., and Vanderbilt, D. Density-matrix electronic-structure method with linear system-size scaling. *Phys. Rev. B* 1993, **47,** 10891–10894; Nunes, R.W., and Vanderbilt, D. Generalization of the density-matrix method to a nonorthogonal basis. *Phys. Rev. B* 1994, **50,** 17611–17614

29. Stephan, U., Drabold, D.A., and Martin, R.M. Improved accuracy and acceleration of variational order-N electronic-structure computations by projection techniques. *Phys. Rev. B* 1998, **58,** 13472–13481.

David A. Drabold, Uwe Stephan, Jianjun Dong, and Serge M. Nakhmanson

The structure of electronic states in amorphous silicon

(a) E = 0.1974 eV; IPR = 658

(b) E = 0.0760 eV; IPR = 92

(c) E = 0.0652 eV; IPR = 126

(d) E = -0.0542 eV; IPR = 24

(e) E = -0.0710 eV; IPR = 18

(f) E = -0.5155 eV; IPR = 7

Color Plate 1. Spatial character of the local-to-extended transition. For a given state of energy E with position as indicated in Fig. 1b, and IPR is the inverse participation ratio; see text), electron charge density is depicted according to color. Each atom shown is colored according the fraction of the total charge at the site: red ($>1/16$), orange ($>1/64$), yellow ($>1/256$), blue ($>1/1\,024$), white ($<1/1\,024$), such that at least 75% of the total charge is shown. The electronic states evolve from the tightly localized (midgap) states (a) to weakly coupled "droplet" states (b) and (c), to fragmented multicluster states (d) and (e), and finally to extended valence states (f).
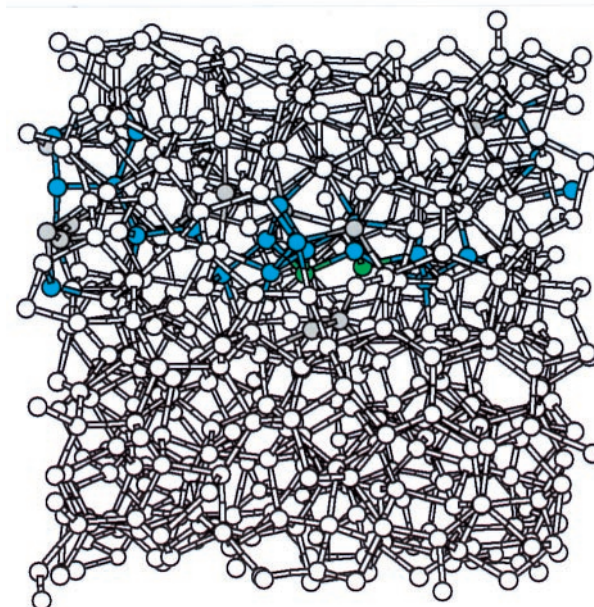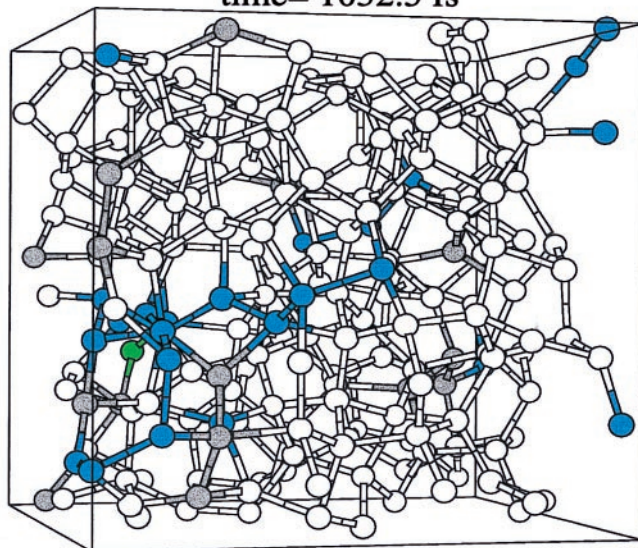
## (a) A snaphot of the LUMO state:
time= 1147.5 fs
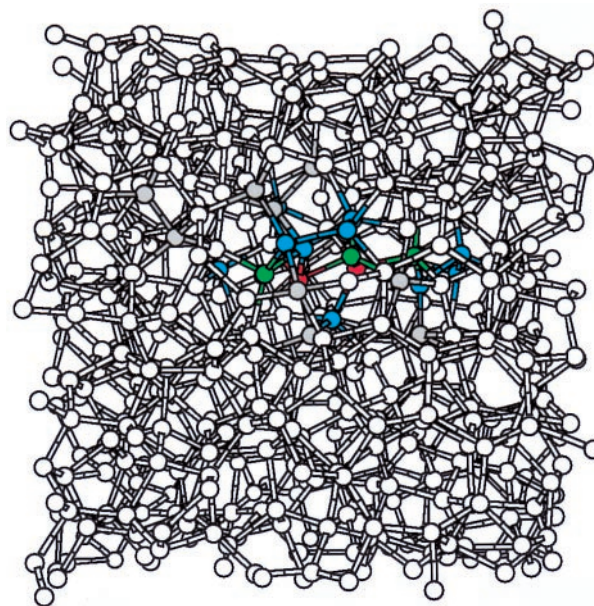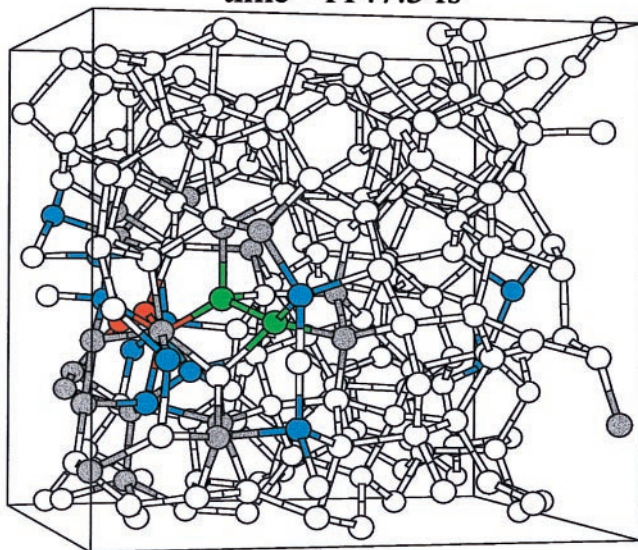
(b) A snaphot of the LUMO state:
time= 1032.5 fs

Color Plate 2. A representation of the LUMO energy eigenstate and the time dependence of its structure, as modulated by thermal disorder for 216 model[2] from 300 K simulation. Color coding reflects different amounts of electron charge on a site: red ($q > 0.1$), green ($0.05 < q < 0.1$), blue ($0.05 < q < 0.01$), gray ($0.01 < q < 0.005$), white ($q < 0.005$). q is the total charge on the site. The charge summed over all sites is unity in all cases. (a) and (b) are "snapshots" from the 2.5-ps simulation. (a) Very localized compact cluster; (b) "stringlike" state, much less localized than in (a). These are only snapshots and depict only the two most commonly recurring structures of the LUMO state.

Color Plate 3. A representation of the HOMO energy eigenstate and the time dependence of its structure, as modulated by thermal disorder for 512 model[2] from 300 K simulation. Same color mapping as Color Plate 2.
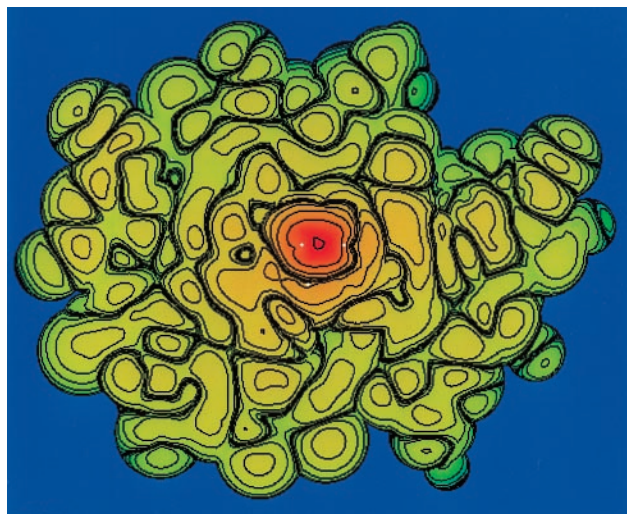
Color Plate 4. Orthonormalized generalized Wannier function for a particularly strained bond in a 4 096-atom model of a-Si,[2] computed with the Sankey[8] Hamiltonian. Here, red depicts maximum charge, green is intermediate, and solid blue is essentially zero charge. White spots are the three atoms that define the plane of the "slice."